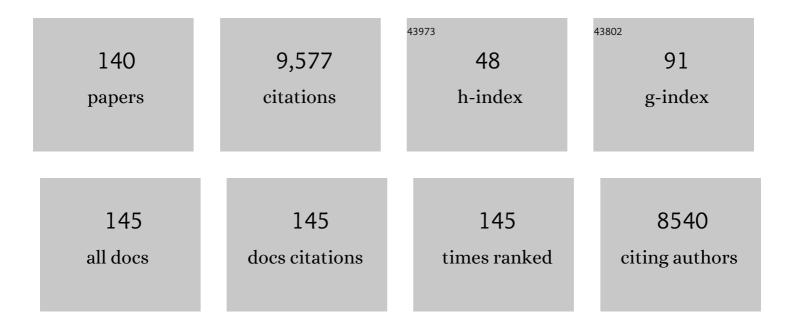
## Michael Garwood

List of Publications by Year in descending order

Source: https://exaly.com/author-pdf/7937001/publications.pdf Version: 2024-02-01



#	Article	IF	CITATIONS
1	The Return of the Frequency Sweep: Designing Adiabatic Pulses for Contemporary NMR. Journal of Magnetic Resonance, 2001, 153, 155-177.	1.2	815
2	Pushing spatial and temporal resolution for functional and diffusion MRI in the Human Connectome Project. NeuroImage, 2013, 80, 80-104.	2.1	769
3	Adiabatic pulses. , 1997, 10, 423-434.		326
4	In vivo quantification of choline compounds in the breast with1H MR spectroscopy. Magnetic Resonance in Medicine, 2003, 50, 1134-1143.	1.9	317
5	Fast and quiet MRI using a swept radiofrequency. Journal of Magnetic Resonance, 2006, 181, 342-349.	1.2	305
6	Neoadjuvant Chemotherapy of Locally Advanced Breast Cancer: Predicting Response with in Vivo1H MR Spectroscopy—A Pilot Study at 4 T. Radiology, 2004, 233, 424-431.	3.6	304
7	9.4T human MRI: Preliminary results. Magnetic Resonance in Medicine, 2006, 56, 1274-1282.	1.9	278
8	MR Imaging Contrast Enhancement Based on Intermolecular Zero Quantum Coherences. , 1998, 281, 247-251.		225
9	Ultrahigh field magnetic resonance imaging and spectroscopy. Magnetic Resonance Imaging, 2003, 21, 1263-1281.	1.0	218
10	Improved tissue cryopreservation using inductive heating of magnetic nanoparticles. Science Translational Medicine, 2017, 9, .	5.8	213
11	Monitoring disease progression in transgenic mouse models of Alzheimer's disease with proton magnetic resonance spectroscopy. Proceedings of the National Academy of Sciences of the United States of America, 2005, 102, 11906-11910.	3.3	193
12	ProtonT2 relaxation study of water, N-acetylaspartate, and creatine in human brain using Hahn and Carr-Purcell spin echoes at 4T and 7T. Magnetic Resonance in Medicine, 2002, 47, 629-633.	1.9	191
13	In vivo visualization of Alzheimer's amyloid plaques by magnetic resonance imaging in transgenic mice without a contrast agent. Magnetic Resonance in Medicine, 2004, 52, 1263-1271.	1.9	181
14	Resolution Improvements inin Vivo1H NMR Spectra with Increased Magnetic Field Strength. Journal of Magnetic Resonance, 1998, 135, 260-264.	1.2	176
15	In Vivo Magnetic Resonance Microimaging of Individual Amyloid Plaques in Alzheimer's Transgenic Mice. Journal of Neuroscience, 2005, 25, 10041-10048.	1.7	150
16	Dental Magnetic Resonance Imaging: Making the Invisible Visible. Journal of Endodontics, 2011, 37, 745-752.	1.4	143
17	Metabolite quantification and highâ€field MRS in breast cancer. NMR in Biomedicine, 2009, 22, 65-76.	1.6	137
18	Adding in Vivo Quantitative1H MR Spectroscopy to Improve Diagnostic Accuracy of Breast MR Imaging: Preliminary Results of Observer Performance Study at 4.0 T. Radiology, 2005, 236, 465-475.	3.6	135

#	Article	IF	CITATIONS
19	Zoomed Functional Imaging in the Human Brain at 7 Tesla with Simultaneous High Spatial and High Temporal Resolution. NeuroImage, 2002, 17, 272-286.	2.1	134
20	Assessment of brain iron and neuronal integrity in patients with Parkinson's disease using novel MRI contrasts. Movement Disorders, 2007, 22, 334-340.	2.2	128
21	Metabolomic Characterization of Human Rectal Adenocarcinoma with Intact Tissue Magnetic Resonance Spectroscopy. Diseases of the Colon and Rectum, 2009, 52, 520-525.	0.7	122
22	Localized <sup>1</sup> H NMR spectroscopy in different regions of human brain <i>in vivo</i> at 7 T: <i>T</i> <sub>2</sub> relaxation times and concentrations of cerebral metabolites. NMR in Biomedicine, 2012, 25, 332-339.	1.6	117
23	Applications of Magnetic Resonance in Model Systems: Tumor Biology and Physiology. Neoplasia, 2000, 2, 139-151.	2.3	110
24	lmaging blood flow in brain tumors using arterial spin labeling. Magnetic Resonance in Medicine, 2000, 44, 169-173.	1.9	109
25	In vivo1H2OT?2 measurement in the human occipital lobe at 4T and 7T by Carr-Purcell MRI: Detection of microscopic susceptibility contrast. Magnetic Resonance in Medicine, 2002, 47, 742-750.	1.9	109
26	Accounting for biological aggregation in heating and imaging of magnetic nanoparticles. Technology, 2014, 02, 214-228.	1.4	102
27	Imaging in breast cancer: Magnetic resonance spectroscopy. Breast Cancer Research, 2005, 7, 149-52.	2.2	100
28	Eliminating spurious lipid sidebands in1H MRS of breast lesions. Magnetic Resonance in Medicine, 2002, 48, 215-222.	1.9	97
29	Observation of resolved glucose signals in1H NMR spectra of the human brain at 4 Tesla. Magnetic Resonance in Medicine, 1996, 36, 1-6.	1.9	87
30	SPION-Enhanced Magnetic Resonance Imaging of Alzheimer's Disease Plaques in AβPP/PS-1 Transgenic Mouse Brain. Journal of Alzheimer's Disease, 2013, 34, 349-365.	1.2	86
31	RASER: A new ultrafast magnetic resonance imaging method. Magnetic Resonance in Medicine, 2007, 58, 794-799.	1.9	85
32	Spectroscopic imaging and spatial localization using adiabatic pulses and applications to detect transmural metabolite distribution in the canine heart. Magnetic Resonance in Medicine, 1989, 10, 14-37.	1.9	81
33	T1ï•MRI contrast in the human brain: Modulation of the longitudinal rotating frame relaxation shutter-speed during an adiabatic RF pulse. Journal of Magnetic Resonance, 2006, 181, 135-147.	1.2	81
34	Transverse relaxation in the rotating frame induced by chemical exchange. Journal of Magnetic Resonance, 2004, 169, 293-299.	1.2	76
35	Predictable Heating and Positive MRI Contrast from a Mesoporous Silica-Coated Iron Oxide Nanoparticle. Molecular Pharmaceutics, 2016, 13, 2172-2183.	2.3	75
36	Magnetic Resonance Imaging of Alzheimer's Pathology in the Brains of Living Transgenic Mice: A New Tool in Alzheimer's Disease Research. Neuroscientist, 2007, 13, 38-48.	2.6	73

#	Article	IF	CITATIONS
37	Localized detection of glioma glycolysis using edited1H MRS. Magnetic Resonance in Medicine, 1993, 30, 18-27.	1.9	71
38	Gapped pulses for frequency-swept MRI. Journal of Magnetic Resonance, 2008, 193, 267-273.	1.2	71
39	Rotating frame relaxation during adiabatic pulses vs. conventional spin lock: simulations and experimental results at 4 T. Magnetic Resonance Imaging, 2009, 27, 1074-1087.	1.0	66
40	Subchronic In Vivo Effects of a High Static Magnetic Field (9.4 T) in Rats. Journal of Magnetic Resonance Imaging, 2000, 12, 122-139.	1.9	65
41	Comparison of amyloid plaque contrast generated by <i>T</i> <sub>2</sub> â€weighted, <i>T</i> â€weighted and susceptibilityâ€weighted imaging methods in transgenic mouse models of Alzheimer's disease. Magnetic Resonance in Medicine, 2009, 61, 1158-1164.	1.9	63
42	SWIFT detection of SPIOâ€labeled stem cells grafted in the myocardium. Magnetic Resonance in Medicine, 2010, 63, 1154-1161.	1.9	61
43	Preparation of Scalable Silicaâ€Coated Iron Oxide Nanoparticles for Nanowarming. Advanced Science, 2020, 7, 1901624.	5.6	61
44	MRI contrast from relaxation along a fictitious field (RAFF). Magnetic Resonance in Medicine, 2010, 64, 983-994.	1.9	59
45	Exchange-influencedT2ïcontrast in human brain images measured with adiabatic radio frequency pulses. Magnetic Resonance in Medicine, 2005, 53, 823-829.	1.9	53
46	Targeting Vascular Amyloid in Arterioles of Alzheimer Disease Transgenic Mice With Amyloid β Protein Antibody-Coated Nanoparticles. Journal of Neuropathology and Experimental Neurology, 2011, 70, 653-661.	0.9	52
47	Quantifying ironâ€oxide nanoparticles at high concentration based on longitudinal relaxation using a threeâ€dimensional SWIFT lookâ€locker sequence. Magnetic Resonance in Medicine, 2014, 71, 1982-1988.	1.9	51
48	Optical and SPION-Enhanced MR Imaging Shows that trans-Stilbene Inhibitors of NF-κB Concomitantly Lower Alzheimer's Disease Plaque Formation and Microglial Activation in AÎ2PP/PS-1 Transgenic Mouse Brain. Journal of Alzheimer's Disease, 2014, 40, 191-212.	1.2	51
49	31P NMR spectroscopy of thein vivo metabolism of an intracerebral glioma in the rat. Magnetic Resonance in Medicine, 1988, 6, 403-417.	1.9	50
50	Magnetic resonance imaging with adiabatic pulses using a single surface coil for RF transmission and signal detection. Magnetic Resonance in Medicine, 1989, 9, 25-34.	1.9	50
51	Asymmetric Adiabatic Pulses for NH Selection. Journal of Magnetic Resonance, 1999, 138, 173-177.	1.2	49
52	MR spectroscopy of breast cancer for assessing early treatment response: Results from the ACRIN 6657 MRS trial. Journal of Magnetic Resonance Imaging, 2017, 46, 290-302.	1.9	49
53	In vivo micro-MRI of intracortical neurovasculature. NeuroImage, 2006, 32, 62-69.	2.1	48
54	Transmural metabolite distribution in regional myocardial ischemia as studied with31p NMR. Magnetic Resonance in Medicine, 1989, 10, 108-118.	1.9	47

#	Article	IF	CITATIONS
55	Continuous SWIFT. Journal of Magnetic Resonance, 2012, 220, 26-31.	1.2	47
56	Electrodeposited Fe and Fe–Au nanowires as MRI contrast agents. Chemical Communications, 2016, 52, 12634-12637.	2.2	47
57	QuantitativeT1ϕand adiabatic Carr-PurcellT2 magnetic resonance imaging of human occipital lobe at 4 T. Magnetic Resonance in Medicine, 2005, 54, 14-19.	1.9	45
58	Selective Contrast Enhancement of Individual Alzheimer's Disease Amyloid Plaques Using a Polyamine and Gd-DOTA Conjugated Antibody Fragment Against Fibrillar Aβ42 for Magnetic Resonance Molecular Imaging. Pharmaceutical Research, 2008, 25, 1861-1872.	1.7	45
59	Functional magnetic resonance imaging using RASER. NeuroImage, 2011, 54, 350-360.	2.1	45
60	Quantitative Assessment of Water Pools by T1p and T2p MRI in Acute Cerebral Ischemia of the Rat. Journal of Cerebral Blood Flow and Metabolism, 2009, 29, 206-216.	2.4	42
61	T2ϕand T1ϕAdiabatic Relaxations and Contrasts. Current Analytical Chemistry, 2008, 4, 8-25.	0.6	41
62	Multi-Band-SWIFT. Journal of Magnetic Resonance, 2015, 251, 19-25.	1.2	41
63	Vitrification and Nanowarming of Kidneys. Advanced Science, 2021, 8, e2101691.	5.6	41
64	Probing Slow Protein Dynamics by Adiabatic <i>R</i> <sub>1Ï</sub> and <i>R</i> <sub>2Ï</sub> NMR Experiments. Journal of the American Chemical Society, 2010, 132, 9979-9981.	6.6	39
65	Detection of calcifications in vivo and ex vivo after brain injury in rat using SWIFT. NeuroImage, 2012, 61, 761-772.	2.1	39
66	Spatially localizedin vivo1H magnetic resonance spectroscopy of an intracerebral rat glioma. Magnetic Resonance in Medicine, 1992, 23, 96-108.	1.9	38
67	On- and off-resonanceT1ÏMRI in acute cerebral ischemia of the rat. Magnetic Resonance in Medicine, 2003, 49, 172-176.	1.9	37
68	Synthesis of Intrinsically Disordered Fluorinated Peptides for Modular Design of Highâ€ <b>S</b> ignal <sup>19</sup> F MRI Agents. Angewandte Chemie - International Edition, 2017, 56, 6440-6444.	7.2	37
69	Effects of continuous localized infusion of granulocyte—macrophage colony—stimulating factor and inoculations of irradiated glioma cells on tumor regression. Journal of Neurosurgery, 1999, 90, 1064-1071.	0.9	36
70	Spinâ€echo MRI using Ï€/2 and Ï€ hyperbolic secant pulses. Magnetic Resonance in Medicine, 2009, 61, 175-187.	1.9	36
71	Intraoral approach for imaging teeth using the transverse <i>B</i> <sub>1</sub> field components of an occlusally oriented loop coil. Magnetic Resonance in Medicine, 2014, 72, 160-165.	1.9	36
72	MRI contrasts in high rank rotating frames. Magnetic Resonance in Medicine, 2015, 73, 254-262.	1.9	36

#	Article	IF	CITATIONS
73	MRI rotating frame relaxation measurements for articular cartilage assessment. Magnetic Resonance Imaging, 2013, 31, 1537-1543.	1.0	35
74	MR Microimaging of amyloid plaques in Alzheimer's disease transgenic mice. European Journal of Nuclear Medicine and Molecular Imaging, 2008, 35, 82-88.	3.3	34
75	Quantification and biodistribution of iron oxide nanoparticles in the primary clearance organs of mice using T <sub>1</sub> contrast for heating. Magnetic Resonance in Medicine, 2017, 78, 702-712.	1.9	34
76	MRI relaxation in the presence of fictitious fields correlates with myelin content in normal rat brain. Magnetic Resonance in Medicine, 2016, 75, 161-168.	1.9	33
77	Role of MRI for detecting micro cracks in teeth. Dentomaxillofacial Radiology, 2016, 45, 20160150.	1.3	32
78	High-field magnetic resonance techniques for brain research. Current Opinion in Neurobiology, 2003, 13, 612-619.	2.0	30
79	Relaxation dispersion in MRI induced by fictitious magnetic fields. Journal of Magnetic Resonance, 2011, 209, 269-276.	1.2	30
80	In Vivo31P and1H NMR studies of rat brain tumor pH and blood flow during acute hyperglycemia: Differential effects between subcutaneous and intracerebral locations. Magnetic Resonance in Medicine, 1989, 12, 219-234.	1.9	29
81	<i>T</i> <sub>1</sub> estimation for aqueous iron oxide nanoparticle suspensions using a variable flip angle SWIFT sequence. Magnetic Resonance in Medicine, 2013, 70, 341-347.	1.9	29
82	Magnetization transfer and adiabatic T1ï•MRI reveal abnormalities in normal-appearing white matter of subjects with multiple sclerosis. Multiple Sclerosis Journal, 2014, 20, 1066-1073.	1.4	29
83	Emerging ethical issues raised by highly portable MRI research in remote and resource-limited international settings. NeuroImage, 2021, 238, 118210.	2.1	28
84	Transformation in Mandibular Imaging With Sweep Imaging With Fourier Transform Magnetic Resonance Imaging. JAMA Otolaryngology, 2011, 137, 916.	1.5	25
85	Quantitative susceptibility mapping detects abnormalities in cartilage canals in a goat model of preclinical osteochondritis dissecans. Magnetic Resonance in Medicine, 2017, 77, 1276-1283.	1.9	25
86	Vitrification and Rewarming of Magnetic Nanoparticle‣oaded Rat Hearts. Advanced Materials Technologies, 2022, 7, 2100873.	3.0	25
87	In vivo observation of lactate methyl proton magnetization transfer in rat C6 glioma. Magnetic Resonance in Medicine, 1999, 41, 676-685.	1.9	24
88	Magnetic Resonance Imaging of Amyloid Plaques in Transgenic Mouse Models of Alzheimers Disease. Current Medical Imaging, 2011, 7, 3-7.	0.4	21
89	Glioma cell density in a rat gene therapy model gauged by water relaxation rate along a fictitious magnetic field. Magnetic Resonance in Medicine, 2012, 67, 269-277.	1.9	21
90	MRI of fast-relaxing spins. Journal of Magnetic Resonance, 2013, 229, 49-54.	1.2	21

#	Article	IF	CITATIONS
91	Detection of neuronal loss using T1ï•MRI assessment of 1H2O spin dynamics in the aphakia mouse. Journal of Neuroscience Methods, 2009, 177, 160-167.	1.3	20
92	MRI by steering resonance through space. Magnetic Resonance in Medicine, 2014, 72, 49-58.	1.9	18
93	Relaxation During Adiabatic Radiofrequency Pulses. Current Analytical Chemistry, 2007, 3, 239-251.	0.6	15
94	In vivo imaging and quantification of iron oxide nanoparticle uptake and biodistribution. , 2012, 8317, .		15
95	Gradientâ€modulated SWIFT. Magnetic Resonance in Medicine, 2016, 75, 537-546.	1.9	15
96	Gradient-Modulated PETRA MRI. Tomography, 2015, 1, 85-90.	0.8	15
97	Uncovering hidden in vivo resonances using editing based on localized TOCSY. Magnetic Resonance in Medicine, 2005, 53, 783-789.	1.9	14
98	Development and Validation of Noninvasive Magnetic Resonance Relaxometry for the In Vivo Assessment of Tissue-Engineered Graft Oxygenation. Tissue Engineering - Part C: Methods, 2016, 22, 1009-1017.	1.1	14
99	Evaluation of (E)-2?-deoxy-2?-(fluoromethylene)cytidine on the 9L rat brain tumor model using MRI. NMR in Biomedicine, 2003, 16, 67-76.	1.6	13
100	Multiparametric MRI of Epiphyseal Cartilage Necrosis (Osteochondrosis) with Histological Validation in a Goat Model. PLoS ONE, 2015, 10, e0140400.	1.1	13
101	Rapid ex vivo imaging of PAIII prostate to bone tumor with SWIFTâ€MRI. Magnetic Resonance in Medicine, 2014, 72, 858-863.	1.9	12
102	Positive contrast from cells labeled with iron oxide nanoparticles: Quantitation of imaging data. Magnetic Resonance in Medicine, 2017, 78, 1900-1910.	1.9	12
103	Transmural distribution of 2-deoxyglucose uptake in normal and post-ischemic canine myocardium. NMR in Biomedicine, 1995, 8, 9-18.	1.6	11
104	The time-dependence of exchange-induced relaxation during modulated radio frequency pulses. Journal of Magnetic Resonance, 2006, 179, 136-139.	1.2	11
105	Designing 3D selective adiabatic radiofrequency pulses with single and parallel transmission. Magnetic Resonance in Medicine, 2018, 79, 701-710.	1.9	11
106	Design of an Intraoral Dipole Antenna for Dental Applications. IEEE Transactions on Biomedical Engineering, 2021, 68, 2563-2573.	2.5	11
107	Imaging and modification of the tumor vascular barrier for improvement in magnetic nanoparticle uptake and hyperthermia treatment efficacy. , 2013, 8584, .		10
108	Establishing the overlap of IONP quantification with echo and echoless MR relaxation mapping. Magnetic Resonance in Medicine, 2018, 79, 1420-1428.	1.9	10

#	Article	IF	CITATIONS
109	Imaging the distribution of iron oxide nanoparticles in hypothermic perfused tissues. Magnetic Resonance in Medicine, 2020, 83, 1750-1759.	1.9	10
110	Contemporary approaches to high-field magnetic resonance imaging with large field inhomogeneity. Progress in Nuclear Magnetic Resonance Spectroscopy, 2020, 120-121, 95-108.	3.9	9
111	Development and validation of 3D MPâ€5SFP to enable MRI in inhomogeneous magnetic fields. Magnetic Resonance in Medicine, 2021, 85, 831-844.	1.9	9
112	<i>B</i> <sub>1</sub> â€gradient–based MRI using frequencyâ€modulated Rabiâ€encoded echoes. Magnetic Resonance in Medicine, 2022, 87, 674-685.	1.9	9
113	Imaging human teeth by phosphorus magnetic resonance with nuclear Overhauser enhancement. Scientific Reports, 2016, 6, 30756.	1.6	8
114	Full analytical solution of the bloch equation when using a hyperbolic-secant driving function. Magnetic Resonance in Medicine, 2017, 77, 1630-1638.	1.9	8
115	Simple partial volume transceive coils for in vivo1H MR studies at high magnetic fields. Concepts in Magnetic Resonance Part B, 2007, 31B, 71-85.	0.3	7
116	Magnetic Resonance Spectroscopy in the Diagnosis and Treatment of Breast Cancer. Seminars in Breast Disease, 2008, 11, 100-105.	0.0	7
117	2D Pulses using spatially dependent frequency sweeping. Magnetic Resonance in Medicine, 2016, 76, 1364-1374.	1.9	7
118	Two-dimensional frequency-swept pulse with resilience to both B1 and B0 inhomogeneity. Journal of Magnetic Resonance, 2019, 299, 93-100.	1.2	7
119	Retrospective correction of surface coil MR images using an automatic segmentation and modeling approach. , 1997, 10, 125-128.		5
120	Frequency offset dependence of adiabatic rotating frame relaxation rate constants: relevance to MRS investigations of metabolite dynamics <i>in vivo</i> . NMR in Biomedicine, 2011, 24, 807-814.	1.6	5
121	Adiabatic pulses. , 0, .		5
122	Phase imaging in brain using SWIFT. Journal of Magnetic Resonance, 2015, 252, 20-28.	1.2	4
123	Noninvasive assessment of tissueâ€engineered graft viability by oxygenâ€17 magnetic resonance spectroscopy. Biotechnology and Bioengineering, 2017, 114, 1118-1121.	1.7	4
124	RF pulse methods for use with surface coils: Frequency-modulated pulses and parallel transmission. Journal of Magnetic Resonance, 2018, 291, 84-93.	1.2	4
125	MRI exploiting frequency-modulated pulses and their nonlinear phase. Journal of Magnetic Resonance, 2020, 318, 106779.	1.2	4
126	Accelerated imaging with segmented 2D pulses using parallel imaging and virtual coils. Journal of Magnetic Resonance, 2019, 305, 185-194.	1.2	3

#	Article	IF	CITATIONS
127	Noninvasive Fluorine-19 Magnetic Resonance Relaxometry Measurement of the Partial Pressure of Oxygen in Acellular Perfluorochemical-loaded Alginate Microcapsules Implanted in the Peritoneal Cavity of Nonhuman Primates. Transplantation, 2020, 104, 259-269.	0.5	3
128	Magnetic Resonance Spectroscopy of Breast Cancer. , 2008, , 407-415.		2
129	What is new in breast MRI spectroscopy. European Journal of Radiology, 2012, 81, S107-S108.	1.2	2
130	Gradient rotating outer volume excitation (GROOVE): A novel method for singleâ€shot twoâ€dimensional outer volume suppression. Magnetic Resonance in Medicine, 2015, 73, 139-149.	1.9	2
131	High-Spatial- and High-Temporal-Resolution Dynamic Contrast-enhanced MR Breast Imaging with Sweep Imaging with Fourier Transformation: A Pilot Study. Radiology, 2015, 274, 540-547.	3.6	2
132	Imaging of a high concentration of iron labeled cells with positive contrast in a rat knee. Magnetic Resonance in Medicine, 2019, 81, 1947-1954.	1.9	2
133	Ultra-low frequency EPR using longitudinal detection and fictitious-field modulation. Journal of Magnetic Resonance, 2020, 321, 106855.	1.2	2
134	Dual polarity encoded MRI using high bandwidth radiofrequency pulses for robust imaging with large field inhomogeneity. Magnetic Resonance in Medicine, 2021, 86, 1271-1283.	1.9	2
135	Exchange-induced relaxation in the presence of a fictitious field. Journal of Magnetic Resonance, 2014, 245, 12-16.	1.2	1
136	3D cine magnetic resonance imaging of rat lung ARDS using gradient-modulated SWIFT with retrospective respiratory gating. , 2015, 9417, .		1
137	UTE-SPECIAL for 3D localization at an echo time of 4Âms on a clinical 3ÂT scanner. Journal of Magnetic Resonance, 2020, 311, 106670.	1.2	1
138	Subchronic In Vivo Effects of a High Static Magnetic Field (9.4 T) in Rats. , 2000, 12, 122.		1
139	Quantifying iron-oxide nanoparticles at high concentration based on longitudinal relaxation using a three-dimensional SWIFT look-locker sequence. Magnetic Resonance in Medicine, 2014, 71, spcone-spcone.	1.9	0
140	Reducing the Complexity of Model-Based MRI Reconstructions via Sparsification. IEEE Transactions on Medical Imaging, 2021, 40, 2477-2486.	5.4	0